Protein Expression and Purification 103 (2014) 28–37

Contents lists available at ScienceDirect

Protein Expression and Purification

journal homepage: www.elsevier.com/locate/yprep

Heterologous expression and physicochemical characterization of a fungal dye-decolorizing peroxidase from *Auricularia auricula-judae*

Dolores Linde [a], Cristina Coscolín [a], Christiane Liers [b], Martin Hofrichter [b], Angel T. Martínez [a], Francisco J. Ruiz-Dueñas [a,*]

[a] Centro de Investigaciones Biológicas, CSIC, Ramiro de Maeztu 9, E-28040 Madrid, Spain
[b] TU Dresden – International Institute Zittau, Markt 23, 02763 Zittau, Germany

ARTICLE INFO

Article history:
Received 13 June 2014
and in revised form 7 August 2014
Available online 18 August 2014

Keywords:
Dye-decolorizing peroxidase
Escherichia coli expression
In vitro activation
Stability properties
Kinetic constants
Biphasic kinetics

ABSTRACT

An efficient heterologous expression system for *Auricularia auricula-judae* dye-decolorizing peroxidase (DyP) has been constructed. DNA coding for the mature protein sequence was cloned into the pET23a vector and expressed in *Escherichia coli* BL21(DE3)pLysS. Recombinant DyP was obtained in high yield as inclusion bodies, and different parameters for its *in vitro* activation were optimized with a refolding yield of ~8.5% of the *E. coli*-expressed DyP. Then, a single chromatographic step allowed the recovery of 17% of the refolded DyP as pure enzyme (1.5 mg per liter of culture). The thermal stabilities of wild DyP from *A. auricula-judae* and recombinant DyP from *E. coli* expression were similar up to 60 °C, but the former was more stable in the 62–70 °C range. Stabilities against pH and H_2O_2 were also measured, and a remarkably high stability at extreme pH values (from pH 2 to 12) was observed. The kinetic constants of recombinant DyP for the oxidation of different substrates were determined and, when compared with those of wild DyP, no important differences were ascertained. Both enzymes showed high affinity for Reactive Blue 19 (anthraquinone dye), Reactive Black 5 (azo dye), 2,2′-azino-bis(3-ethylbenzothiazoline-6-sulfonic acid) and 2,6-dimethoxyphenol, with similar acidic pH optima and oxidative stabilities. Oxidation of veratryl alcohol and a nonphenolic lignin model dimer were confirmed, although as minor enzymatic activities. Interestingly, two sets of kinetic constants could be obtained for the oxidation of Reactive Blue 19 and other substrates, suggesting the existence of more than one oxidation site in this new peroxidase family.

Introduction

Heme peroxidases include a large number of enzymes containing heme as a prosthetic group. These enzymes catalyze the oxidation of a wide range of substrates using hydrogen peroxide or organic hydroperoxides as electron acceptors. Heme peroxidases are found in all kingdoms of life and are involved in a wide range of biological processes such as defense mechanism, immune response, pathogenicity, detoxification or biomass degradation. They were traditionally classified based on their sequence similarities and structural properties into the two large superfamilies of animal and plant–fungal–bacterial peroxidases, the latter divided into class I (prokaryotic), class II (fungal) and class III (plant) peroxidases [1]. For a long time, this classification included most of the known heme peroxidases. However, currently there are new heme peroxidases characterized and many others identified in genome sequences which do not fit into the above two superfamilies. These peroxidases have been grouped into the new (super)family of hemethiolate peroxidases secreted by fungi, comprising chloroperoxidase from *Leptoxyphium fumago* and the unspecific peroxygenase from *Agrocybe aegerita*, among others [2]; and into the family of dye-decolorizing peroxidases (DyP[1]) widespread in fungi and bacteria [3], which has been suggested to form the CDE structural

* Corresponding author. Fax: +34 915360432.
E-mail address: fjruiz@cib.csic.es (F.J. Ruiz-Dueñas).

[1] *Abbreviations used:* ABTS, 2,2′-azino-bis(3-ethylbenzothiazoline-6-sulfonate); B&R buffer, Britton–Robinson buffer; CDS, coding DNA sequence; DMP, 2,6-dimethoxyphenol; DTT, dithiothreitol; DyP, dye-decolorizing peroxidase; DyP*, recombinant DyP; EDTA, ethylenediaminetetraacetic acid; GSH, reduced glutathione; GSSG, oxidized glutathione; HPLC, high-performance liquid chromatography; IPTG, isopropyl-β-D-thiogalactopyranoside; k_{app}, apparent second-order inactivation rate constant; k_{cat}, catalytic constant; k_i, first-order inactivation rate constant; K_I, H_2O_2 concentration that results in the half maximum inactivation rate of the enzyme; K_m, Michaelis–Menten constant; k_{obs}, pseudo first-order inactivation rate constant; LiP, lignin peroxidase; MnP, manganese peroxidase; pI, isoelectric point; SDS–PAGE, sodium dodecyl sulfate–polyacrylamide gel electrophoresis; T_{50}, 50% inactivation temperature; TB medium, Terrific Broth medium; VA, veratryl alcohol; VP, versatile peroxidase.

http://dx.doi.org/10.1016/j.pep.2014.08.007
1046-5928/

superfamily together with the microbial chlorite dismutase and EfeB heme families [4].

The first time that peroxidase and specific dye-decolorizing activities were related was in crude extracellular enzyme preparations from liquid cultures of a strain of the fungus *Bjerkandera adusta* [5] (it appears in the literature first described as *Geotrichum candidum* and then misidentified by molecular methods as *Thanathephorus cucumeris* as explained by Ruiz-Dueñas et al. [6]). This DyP was purified and characterized as a heme protein (Soret band at 406 nm) of high molecular weight (60 kDa) with a substrate specificity that differs from that of the members of the well-known superfamily of plant–fungal–bacterial peroxidases, including recalcitrant anthraquinone dyes among the compounds it is able to efficiently oxidize [7]. Then several DyP isoenzymes were described in this fungus and the coding gene for one of them was cloned, sequenced [8] and heterologously expressed as an active and soluble enzyme in both *Aspergillus oryzae* [9] and *Escherichia coli* [10], although with low yields after laborious purification processes requiring several chromatographic steps.

Until June 2014, the Peroxibase database (http://peroxibase.toulouse.inra.fr) had registered 233 DyP sequences, mainly inferred from bioinformatic analysis of sequenced genomes, which have been classified into four types. Type A includes 26 sequences of bacterial DyPs; type B gathers 45 sequences from bacteria, ascomycota and the only DyP sequence from a non-fungal eukaryote (the mycetozoon *Dictyostelium discoideum*); type C groups 24 sequences from bacteria, and two sequences from *B. adusta*; and type D includes 138 fungal sequences from ascomycota (26) and basidiomycota (112). The fact that DyP-type peroxidases have been found in bacteria and eukaryota is of great relevance because this means that the ancient root of these enzymes appeared before the branching of the two organism superkingdoms (domains). In contrast, the ancestor of ligninolytic peroxidases (in class II of the plant–fungal–bacterial peroxidase superfamily) would have appeared around the end of the Carboniferous period as part of the lignin-degrading machinery of the Agaricomycetes ancestor [11]. Although DyP genes also expanded in the genomes of lignin-degrading basidiomycetes [12] and lignin model compounds can be oxidized by DyPs [13], the appearance and evolutionary history of DyPs is very different from that of class II ligninolytic peroxidases. Therefore, and as mentioned above, DyPs have been classified in a heme peroxidase superfamily apart from the animal and plant–fungal–bacterial peroxidase superfamilies [2,3,14,15].

Despite the high number of putative DyP sequences deposited at protein databases, only a modest number of bacterial DyPs from *Bacteroides thetaiotaomicron*, *Shewanella oneidensis* [16], *Anabaena* sp. [17], *E. coli* [18], *Thermobifida fusca* [19], *Rhodococcus jostii* [20], *Amycolatopsis* sp. [21], *Pseudomona aeruginosa* [22], *Bacillus subtilis* and *Pseudomonas putida* [23], and fungal DyPs from *B. adusta* [5], *Termitomyces albuminosus* [24], *Marasmius scorodonius* [25], *A. auricula-judae* [26], *Irpex lacteus* [27], *Exidia glandulosa* and *Mycena epipterygia* [13] have been purified and characterized to date, some of them as several isoenzymes. One of the most attractive characteristics of DyPs is their resistance to elevated temperatures, pressures [28] and acidic conditions [26]. Moreover, DyPs oxidize dyes that are not good substrates for other peroxidases [13,26], differ from them in their molecular structure [16,29,30] and their catalytic mechanisms are still largely unknown. For the systematic investigation of these peroxidases, the development of appropriate over-expression methods that allow their production as recombinant proteins will be essential. An optimized expression system is required to obtain protein variants by site-directed mutagenesis that allow both evaluation of structure–function relationships in this enzyme family and the catalytic and stability improvement for their future biotechnological application.

In the present study, a system for *A. auricula-judae* DyP (isoform I) heterologous expression in *E. coli* has been developed. Since recombinant DyP (DyP*) was produced in high quantity as inclusion bodies, *in vitro* folding and purification conditions were optimized, and the catalytic and stability properties of the purified enzyme were determined and compared with those of the wild enzyme isolated from fungal cultures.

Materials and methods

Materials

Yeast extract and bactopeptone were from Difco. Ampicillin, chloramphenicol, dithiotreitol (DTT), lysozyme and hemin were from Sigma–Aldrich. 2,2′-Azino-bis(3-ethylbenzothiazoline-6-sulfonic acid) (ABTS) and DNaseI were from Boehringer Mannhein. *Nde*I and *Bam*HI restriction enzymes were from New England Biolabs. All other chemicals were from Merck.

The mature protein-coding DNA sequence (CDS) (GenBank accession No. JQ650250) of *A. auricula-judae* DyP (isoform I) (described as *Aj*PI) [13,26] with additional *Nde*I and *Bam*HI restriction sites at the 5′ and 3′ ends, respectively, was synthesized by ATG:biosynthetics (Merzhausen, Germany) after codon optimization for *E. coli* expression.

Fungal DyP production and purification

Wild (non recombinant) isoform I of *A. auricula-judae* DyP was produced in complex liquid media based on tomato juice [26]. After concentration and ultrafiltration (10-kDa cutoff) of the enzyme containing culture liquid, the crude DyP preparation was purified by three steps of fast protein liquid chromatography (FPLC, Äkta Explorer, GE HealthCare Europe GmbH, Freiburg, Germany) using anion exchange (Q Sepharose and Mono Q) and chromatofocusing techniques as described previously [26]. The purified DyP was dialyzed against 10 mM sodium tartrate (pH 5) and stored at −80 °C.

Vector construction and DyP heterologous production in E. coli

DyP CDS was excised from the pGH vector (provided by ATG:biosynthetics, Merzhausen, Germany) at the *Nde*I and *Bam*HI sites, and cloned into the expression vector pET23a (Novagen) encoding ampicillin resistance to yield the pET23a-DyPI plasmid. Then it was transformed into *E. coli* DH5α for amplification, confirmed by DNA sequencing (using an ABI 3730 DNA Analyzer of Applied Biosystems) and introduced into *E. coli* BL21(DE3)pLysS, carrying a chloramphenicol resistance maker, for subsequence heterologous expression.

For DyP* production, *E. coli* BL21(DE3)pLysS cells containing the pET23a-DyPI vector were grown overnight at 37 °C and 170 rpm in 500 mL flasks containing 200 mL of Luria Bertani broth (LB) supplemented with 100 μg/mL of ampicillin and 34 μg/mL of chloramphenicol. The precultured cells were used to inoculate 2 L flasks containing 1 L of Terrific Broth (TB) supplemented with ampicillin and chloramphenicol, that were grown for 3 h at 37 °C and 200 rpm (OD_{600nm} ~0.6). The cultures were induced with 1 mM IPTG, grown for a further 4 h and then harvested by centrifugation. Protein expression was monitored by sodium dodecyl sulfate–polyacrylamide gel electrophoresis (SDS–PAGE). For that, the cells from 1 mL *E. coli* cultures were harvested, resuspended in 50 μL of loading buffer and boiled. SDS–PAGE was performed in 12% polyacrylamide gels using dual color precision plus protein (Bio-Rad) as standard and Coomassie R-250 staining.

The bacterial pellet corresponding to 5 L of culture was resuspended in 50 mM Tris–HCl (pH 8.0) containing 10 mM

ethylenediaminetetraacetic acid (EDTA) and 5 mM DTT (lysis buffer), and the mixture was incubated with 2 mg/mL lysozyme for 1 h on ice. Then 0.1 mg/mL of DNaseI was added and incubated for another 30 min. The solution was sonicated (1 min for three times with intervals on ice) and centrifuged 1 h at 15,000 rpm. The pellet containing the DyP polypeptide inclusion bodies was washed with 20 mM Tris–HCl (pH 8.0) containing 1 mM EDTA and 5 mM DTT. The protein was solubilized in 10 mL of 50 mM Tris–HCl (pH 8.0) containing 8 M urea, 1 mM EDTA and 5 mM DTT, gently stirred for 1 h at 4 °C to complete solubilization of the DyP polypeptide, and centrifuged for 15 min at 15,000 rpm to eliminate insoluble debris. Protein concentration was determined by the Bradford method using the Protein Assay (Bio-Rad), and bovine serum albumin as standard.

*In vitro activation of DyP**

To investigate the optimal activation conditions for DyP protein, initial folding assays were performed in 200 μL volume using 96-well plates. The parameters varied included pH (5–9.5), GSSG (oxidized glutathione) (0–1.5 mM), hemin (0–30 μM) and urea (0.1–0.8 M). The protein (0.1 mg/mL), DTT (0.02 mM) and EDTA (0.1 mM) concentrations remained constant in these assays. Folding was assayed both at 4 and 25 °C. Once these parameters were fixed, the optimal folding time was investigated for 7 days.

After *in vitro* activation, incorrectly folded protein was eliminated by centrifugation (45 min at 2000 rpm) and folding efficiency was estimated by the ABTS oxidation assay described below. Aliquots from the different folding assays were transferred to a new 96-well plate, and carried to a final volume of 200 μL with 0.5 mM ABTS in 50 mM sodium tartrate prepared at the same pH (4.5) previously used to determine the wild DyP activity on this substrate [26]. Reaction was initiated with 0.1 mM H_2O_2, and monitored at 436 nm in a microplate reader (Spectra max plus 384, Molecular Devices) using the molar absorption coefficient provided below.

Larger scale folding was performed using the optimized conditions found in the small-scale experiments. These conditions included: 50 mM phosphate (pH 6), 0.1 mM EDTA, 0.02 mM DTT, 10 μM hemin, 0.1 mg/mL protein, 0.2 M urea, and 4 °C incubation. After 144 h, the mixture was concentrated (Pellicon and Amicon, using 10 kDa cut-off membranes). The concentrated sample was dialyzed against 20 mM sodium acetate (pH 4.3) to promote the precipitation of free hemin and aggregates of misfolded protein. The insoluble material was eliminated by centrifugation at 13,000 rpm for 30 min. The supernatant including active DyP* was dialyzed against 10 mM Tris–HCl (pH 7) for subsequent purification.

DyP purification and characterization*

DyP* was purified by ion-exchange chromatography in a Resource Q column (GE Healthcare) coupled to an ÄKTA fast protein liquid chromatography system. The activated enzyme obtained as described above was loaded onto the column in 10 mM Tris–HCl (pH 7) (1 mL/min). The correctly folded protein and the misfolded forms retained at pH 7 were eluted with a NaCl gradient from 0 to 0.3 M. Those fractions containing the correctly folded DyP* were pooled, concentrated, dialyzed against storage buffer (10 mM sodium tartrate, pH 5) and stored at −80 °C.

DyP* was analyzed by SDS–PAGE, as described above, to confirm the purity of the protein. Absorption spectra were recorded in 10 mM sodium tartrate (pH 5) at 25 °C (conditions in which the enzyme is stable and catalytically active) in a Thermo Spectronic UV–visible spectrophotometer. The molar absorption coefficient of DyP* ($\varepsilon_{405\ nm}$ 117,000 $M^{-1}\,cm^{-1}$) was calculated from a triplicate Bradford determination of pure protein concentration, and used to estimate enzyme concentrations. Enzyme reduction was achieved by adding 5 mM sodium dithionite to 5 μM enzyme in 10 mM sodium tartrate (pH 5).

The isoelectric point (pI) of the desalted protein was determined by isoelectrofocusing (IEF) in gels with 5% polyacrylamide and a mixture of Ampholines to obtain a pH range of 2.5–5 (mixing 85% from pH 2.5 to 5 and 15% from pH 3 to 10 (GE Healthcare)), with 1 M H_3PO_4 and 1 M NaOH in anode and cathode, respectively. Proteins were stained for peroxidase activity with 2.5 mM ABTS and 0.1 mM H_2O_2 in 100 mM sodium tartrate, pH 4.5.

Effect of peroxide on DyP activity

The effect of peroxide on DyP half-life, defined as the time (in min) at which 50% of activity is lost, was calculated by incubating 1 μM DyP* in 10 mM sodium tartrate (pH 5) containing 1 or 3 mM H_2O_2 (representing 1000 and 3000 equivalents, respectively). The remaining activity at several incubation times was measured with 2.5 mM ABTS in 100 mM sodium tartrate (pH 3) (optimum pH), as described below. The inactivation constants were calculated as described by Hernández-Ruiz et al. [31].

The time course of 1 μM (wild or recombinant) enzyme inactivation in 10 mM sodium tartrate (pH 5) in the presence of 0–30,000 M equivalents of peroxide at 4 °C was followed (in triplicate reactions). The enzyme incubated under the same experimental conditions in absence of H_2O_2 was used as a reference, and its activity at the beginning of the experiment was considered to be 100%.

The data of residual activity *vs* time at each H_2O_2 concentration were fitted to an exponential decay model and a pseudo first-order inactivation rate constant (k_{obs}, s^{-1}) was obtained. The k_{obs} values were fitted to a hyperbolic function by a non-linear least-squares fitting. From this function a first-order inactivation rate constant (k_i) and the H_2O_2 concentration that results in the half maximum inactivation rate of the enzyme (K_I), were obtained. Fitting of k_i and K_I to the normalized equation $k_{obs} = ((ki/K_I)\ [H_2O_2])/(1 + [H_2O_2])/K_I)$ yielded the apparent second order inactivation rate constant ($k_{app} = k_i/K_I$) with its corresponding standard error. The fitting was calculated with SigmaPlot (version 11.0).

Effect of pH and temperature on DyP activity

The optimum pH of the wild and recombinant DyPs oxidizing Reactive Blue 19 (50 μM), ABTS (500 μM), 2,6-dimethoxyphenol (DMP, 500 μM), Reactive Black 5 (25 μM) and veratryl alcohol (VA, 10 mM) was measured in 50 mM Britton–Robinson (B&R) buffer of pH 2–12 (in triplicate reactions), as described below. The activity at the optimum pH was considered to be 100%.

The pH stability was determined by incubating the two enzymes for 24 h in 50 mM KCl–HCl (pH 1) or B&R buffer (pH 2–12) at 25 or 4 °C. The remaining activity at several incubation times was measured with 2.5 mM ABTS in 100 mM sodium tartrate (pH 3) (in triplicate reactions), as described below. The activity immediately after adding the enzyme to the buffer was taken as 100%.

To evaluate their temperature stability, the two enzymes in sodium tartrate 10 mM (pH 5) were incubated in the range from 25 to 80 °C. After 10 min, they were allowed to rest for 2 min at 4 °C, and the remaining activities measured with 2.5 mM ABTS in 100 mM sodium tartrate (pH 3) in triplicate reactions. The T_{50} values, defined as the temperature at which 50% of activity is lost in a 10-min incubation, were calculated.

Enzymatic activities: kinetic analyses

Steady-state kinetic constants of the wild and recombinant DyPs were determined spectrophotometrically using a Thermo

Spectronic UV–visible spectrophotometer at 25 °C. For DMP, ABTS and VA oxidation, absorbance increases at 469 nm (dimeric coerulignone; ε_{469} = 55,000 M^{-1} cm^{-1}), 436 nm (ABTS cation radical; ε_{436} = 29,300 M^{-1} cm^{-1}) and 310 nm (veratraldehyde; ε_{310} = 9300 M^{-1} cm^{-1}) were followed, respectively. Absorbance decreases were followed in the case of Reactive Black 5 (ε_{598} = 30,000 M^{-1} cm^{-1}) and Reactive Blue 19 (ε_{595} = 10,000 M^{-1} cm^{-1}) oxidation resulting in dye decolorization. All the substrates were tested using the enzymes at a final concentration of 10 nM (except VA whose oxidation was assayed with 100 nM enzyme) and a 0.1 mM concentration of H_2O_2.

The plotting and analysis of the curves was carried out using SigmaPlot (version 11.0). Apparent affinity constant (Michaelis–Menten constant, K_m), turnover number (catalytic constant, k_{cat}) and their standard errors were obtained by non-linear least-squares fitting of the experimental measurements to the Michaelis–Menten model. The catalytic efficiency (k_{cat}/K_m) values with their standard errors were calculated fitting the experimental data to the normalized Michaelis–Menten equation: $v = (k_{cat}/K_m)[S]/(1 + [S]/K_m)$. When no-saturation kinetics was observed (i.e. VA oxidation), the catalytic efficiency value was calculated as the slope of the straight line obtained from the representation of the initial velocities (s^{-1}) *vs* substrate concentration. Two sets of steady-state kinetic constants were calculated for the oxidation of some of the substrates assayed: (i) DMP in the 4–60 and 200–8000 μM ranges; and (ii) Reactive Blue 19 in the 0.2–10 and 50–270 μM ranges.

Oxidation of lignin model dimer

Enzymatic oxidation of the racemic (*erythro* plus *threo*) non-phenolic lignin model dimer 4-*O*-methylsyringylglycerol β-guaiacyl ether (provided by J. Sipilä and P. Nousiainen from Helsinki University) was followed by high-performance liquid chromatography (HPLC). The reaction mixture (0.3 mL) contained 1 mM dimer, 0.3 mM H_2O_2, 17 μM of enzyme in pH 2.5 B&R buffer, and was stirred at 700 rpm and 25 °C for 16 h.

The reaction products were analyzed using an Agilent HPLC equipment fitted with a Zorbax Eclipse XDB-C18 column (of 4.6 × 150 mm) and methanol:water containing 0.1% formic acid (v/v) as mobile phase (35:65 for 15 min, followed by 50:50 for 30 min) at a flow rate of 1 mL min^{-1} at room temperature. Elution was monitored at 255 nm. 3,4,5-Trimethoxybenzaldehyde (1 mM) was used as standard for retention time and response factor calculation.

Results and discussion

High-yield E. coli production of A. auricula-judae DyP

The pET23a-DyPI vector containing the CDS for the mature DyP (isoform I) of *A. auricula-judae*, optimized for expression in *E. coli*, was introduced into the BL21(DE3)pLysS strain. Its expression at small-scale (15 mL cultures) was checked in time course experiments using two different media (LB and TB) and temperatures (16 and 37 °C), and the recombinant protein mainly accumulated as inclusion bodies. The highest protein production, estimated by SDS–PAGE, was attained 4 h after 1 mM IPTG induction in TB medium at 37 °C.

Larger-scale production of DyP* was performed in 5 L of TB medium (distributed in 2-L flasks containing 1 L/flask). After 4 h induction with IPTG, cell harvesting and lysing, it was determined that large quantities of protein (about 100 mg/L) accumulated in insoluble inclusion bodies as previously observed in the small-scale experiments. Then, conditions for DyP* *in vitro* activation were optimized, as described for other peroxidases [32–37].

*In vitro activation of DyP**

The DyP* inclusion bodies were solubilized in 8 M urea, and used as starting point of folding optimization experiments. The following parameters were simultaneously varied in 96-well microplates: hemin and urea concentration, GSSG/GSH ratio, and pH. The folding efficiency was followed by DyP activity measured as ABTS oxidation. In the subsequent experiments the above folding parameters were adjusted and the influence of the time and temperature folding investigated.

The effect of pH on DyP folding was explored between pH 5 and 9.5 (Fig. 1A) and the optimum was found at pH 6, a value far from the pH 9.5 reported for the *M. scorodonius* DyP [33]. No GSSG addition was required for DyP folding, most probably because its sequence includes a single cysteine residue and no disulfide bond formation is needed. Optimal activity was achieved for hemin 5–10 μM (assayed range was from 0 to 30 μM) (Fig. 1B) corresponding to ~2–5-fold molar excess respect to the protein (2.1 μM). The urea concentration for an optimum folding was found at 0.2 M (Fig. 1C). It is important to mention that between the initial 8 M urea concentration, in which the inclusion bodies were solubilized, and the final 0.2 M of the folding mixture, an intermediate step was performed in which the protein was dissolved in 1.5 M urea. The folding mixture was maintained at 4 or 25 °C, and the optimum was found at 4 °C (Fig. 1D) as previously described for the recombinant DyP from *M. scorodonius* [33]. The experiment was performed at both temperatures for 7 days, attaining the maximal recovery of folded active DyP* after 6 days (Fig. 1D).

*Purification of DyP**

For enzyme purification, large-scale (5 L culture) activation of the *E. coli*-expressed DyP* protein was carried out under the previously optimized conditions, i.e. folding in 50 mM phosphate (pH 6), containing 10 μM hemin, 0.2 M urea and 1 mg/mL protein, for 6 days at 4 °C. The mixture was concentrated, dialyzed and centrifugated, allowing the elimination of folding additives and unfolded protein, yielding a supernatant with 10-fold purification factor. Then, DyP* was purified by a single anion exchange-chromatographic step, using a Resource Q column (Fig. 2A), in a process that significantly differed from that optimized for the wild enzyme from *A. auricula-judae* cultures consisting in three different chromatographic steps (Table 1). The SDS–PAGE analysis of the purified DyP* shows a single band of protein (Fig. 2A, inset) that, due to the lack of glycosylation machinery in *E. coli*, has a molecular weight slightly lower than that of the wild DyP purified from the fungal cultures (51 kDa) [26], but in agreement with that calculated from the amino-acid sequence (47 kDa). On the other hand, the experimentally determined DyP* isoelectric point (pI = 4.4) was near that of the fungal DyP (pI = 4.3). The spectra of the resting ferric states of recombinant and wild enzymes were also obtained (Fig. 2B). Their analysis revealed that both enzymes exhibit a typical peroxidase spectrum [38] with no significant differences between them. The Soret band was observed at 406 nm together with two small maxima at 506 and 532 nm corresponding to the charge transfer bands CT2 and CT1, respectively. The subsequent addition of an excess of dithionite resulted in a shift of the Soret band to 420 nm and appearance of prominent bands at 540 and 570 nm (Fig. 2B) as a consequence of the ferric heme reduction to the ferrous form in both DyP* and wild DyP.

Optimization of the *in vitro* folding and purification of DyP* allowed recovering 1.5% of the DyP expressed in *E. coli*, resulting from 8.5% to 17% folding and purification yields, respectively

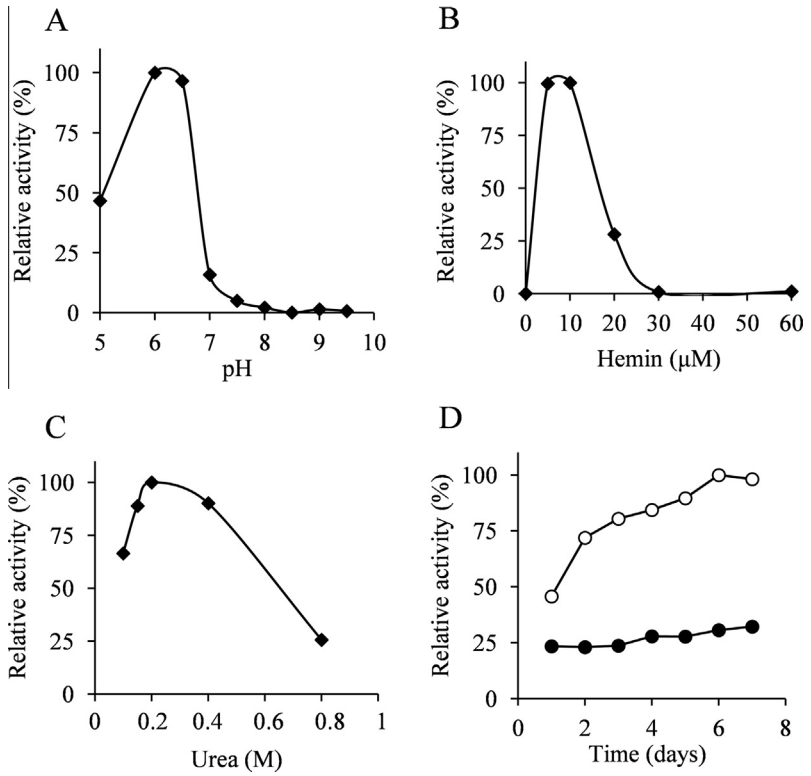

Fig. 1. Optimization of *in vitro* folding parameters. (A) Effect of pH (24 h of incubation at 4 °C, 10 μM hemin, and 0.15 M urea). (B) Effect of hemin concentration (24 h of incubation at 4 °C, pH 6, and 0.15 M urea). (C) Effect of urea concentration (24 h of incubation at 4 °C, pH 6, and 10 μM hemin). (D) Effect of temperature (white circles, 4 °C; and black circles, 25 °C) and time (pH 6, 10 μM hemin, and 0.15 M urea). No GSSG was added. The extent of folding is shown as percentage of the maximal activity obtained using ABTS as substrate.

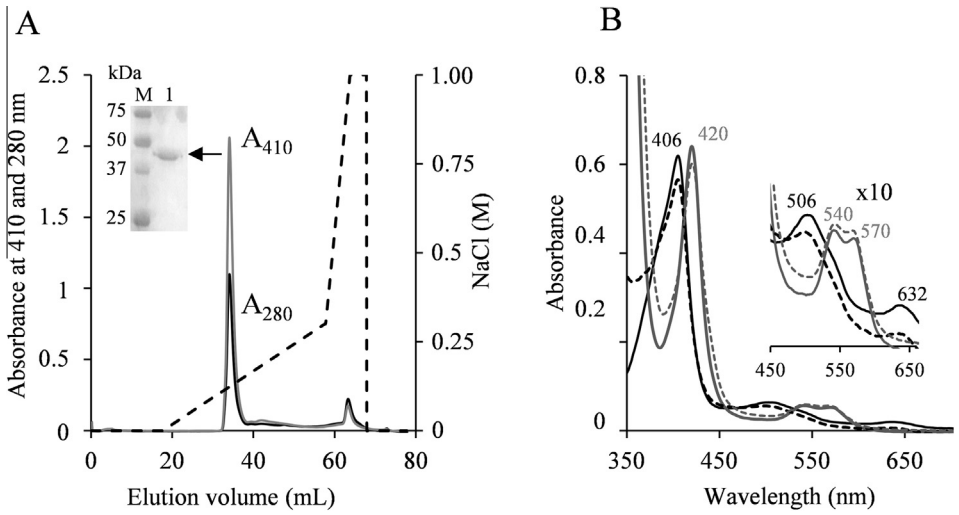

Fig. 2. Purification of refolded DyP* and spectral analysis compared with the wild enzyme. (A) Resource Q chromatogram showing the DyP* elution profile at 280 and 410 nm, and the NaCl gradient. The inset shows SDS–PAGE of the purified DyP* (lane 1) and molecular-mass markers (lane M). (B) Electronic absorption spectra of DyP* (continuos line) and wild DyP from fungal cultures (dashed line). The enzyme spectra at 5 μM concentration in 10 mM sodium tartrate, pH 5, correspond to the resting state (ferric) (black) and the reduced (ferrous) form obtained by addition of 5 mM dithionite (grey).

(Table 1), which corresponds to 1.5 mg protein per liter of culture. These values are similar to those obtained for *E. coli*-expressed and *in vitro* folded versatile peroxidase (VP) of *Pleurotus eryngii* (5.50 mg/L) [34], lignin peroxidase (LiP) of *Trametes cervina* (0.38 mg/L) [32] or manganese peroxidase (MnP) of *Phanerochaete chrysosporium* (0.28 mg/L) [37]. The prokaryotic DyPs of *Anabaena* sp. [17] and *T. fusca* [19] and the fungal DyP of *B. adusta* [10] were successfully expressed in *E. coli* as soluble proteins. In these studies, three chromatographic steps were needed to obtain 0.11 mg of *B. adusta* DyP and 10 mg of *Anabaena* DyP per liter of culture, while one step (using Ni^{2+}-NTA agarose) allowed purification of 3 mg of His-tagged *T. fusca* DyP per liter of culture. The His-tagged DyP of *M. scorodonius* was also expressed with high yield in *E. coli* as inclusion bodies and *in vitro* folded obtaining 0.4 mg of purified enzyme

Table 1
Purification of *E. coli* expressed *A. auricula-judae* DyP (isoform I) after *in vitro* activation (from a 1-L culture), and wild DyP (*Aj*PI) isolated from *A. auricula-judae* (from a 1-L culture) [26].

		Protein (mg)	Total activity (U)	Specific activity (U/mg)	Yield (%)	Purification (folds)
DyP*	Folding mixture	100,0	2,130	21	100	1
	Dialysis	3.0	540	180	25	8
	Resource Q	1.5	370	247	17	12
Wild DyP (*Aj*PI)	Culture liquid	78.0	2,220	28.4	100	1
	Ultrafiltration	58.0	2,060	35.5	93	1
	Q Sepharose	12.8	2,030	158.0	92	6
	Mono Q	2.1	978	465.0	44	16
	Mono P	2.0	938	469.0	42	17

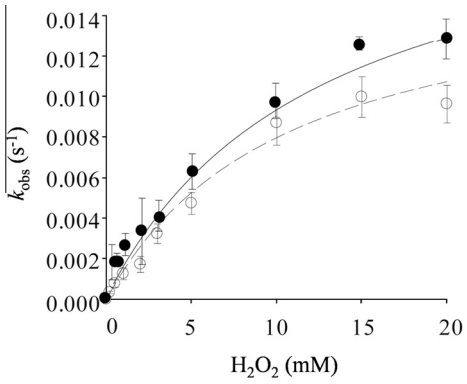

Fig. 3. H_2O_2 inactivation kinetics. Plots of pseudo first-order inactivation rate constants (k_{obs}) *vs* H_2O_2 concentrations of DyP* from *E. coli* (white circles) and wild DyP from *A. auricula-judae* (black circles).

per liter of culture [33]. The *A. auricula-judae* enzyme is the only DyP overexpressed in *E. coli* (as inclusion bodies) and successfully activated and purified without any fusion peptide.

Oxidative inactivation by peroxide

The loss of DyP (fungal and *E. coli* expressed) catalytic activity in the presence of H_2O_2 (and absence of reducing substrate) was determined by measuring the residual activity with ABTS, and inactivation constants were calculated. The time course of residual activity, expressed as percentage of the initial activity in presence of 0–30,000 peroxide equivalents, fits to an exponential decay equation: $f = y_0 + ae^{(-bx)}$, where b is the k_{obs} or pseudo first-order inactivation rate constant calculated for each H_2O_2 concentration. The hyperbolic nature of the plot obtained for k_{obs} *vs* H_2O_2 concentration (Fig. 3) demonstrates the saturation kinetic of the enzyme inactivation by peroxide.

All heme peroxidases are inactivated by H_2O_2 in absence of reducing substrates. The effect of peroxide on different molecular events such as loss of iron coordination, heme destruction or protein multimerization has been previously reported for these enzymes [39]. For fungal and *E. coli*-expressed DyP the first-order inactivation rate constant, k_i ($0.019 \pm 0.004\ s^{-1}$ and $0.016 \pm 0.003\ s^{-1}$, respectively), the H_2O_2 concentration that results in the half maximal inactivation rate to 1 μM enzyme, K_I (12.9 ± 5.0 and 10.5 ± 3.7 mM, respectively), and the apparent second-order inactivation rate constant, k_{app} (1.5 ± 0.4 and $1.5 \pm 0.3\ M^{-1}\ s^{-1}$, respectively) were calculated. No oxidative stability differences were found among them. Considering the above k_{app} values, DyP would be more stable than horseradish peroxidase, an enzyme well characterized from the point of view of oxidative stability, whose different isoenzymes show higher k_{app} values ($3.1–5.0\ M^{-1}\ s^{-1}$), even at lower k_i values ($0.005–0.010\ s^{-1}$) [40].

The half-life of *A. auricula-judae* DyP* was 38 min in the presence of 1000 peroxide equivalents (1 mM) and 3.8 min in presence of 3000 equivalents (3 mM). The half-life in the presence of 1 mM peroxide has been reported for other fungal peroxidases, and varies from 1.3 min for VP, 6.2 min for LiP, 8.5 min for MnP, and 115 min for chloroperoxidase, but comparison is difficult because the enzyme concentration is not reported in these studies [39].

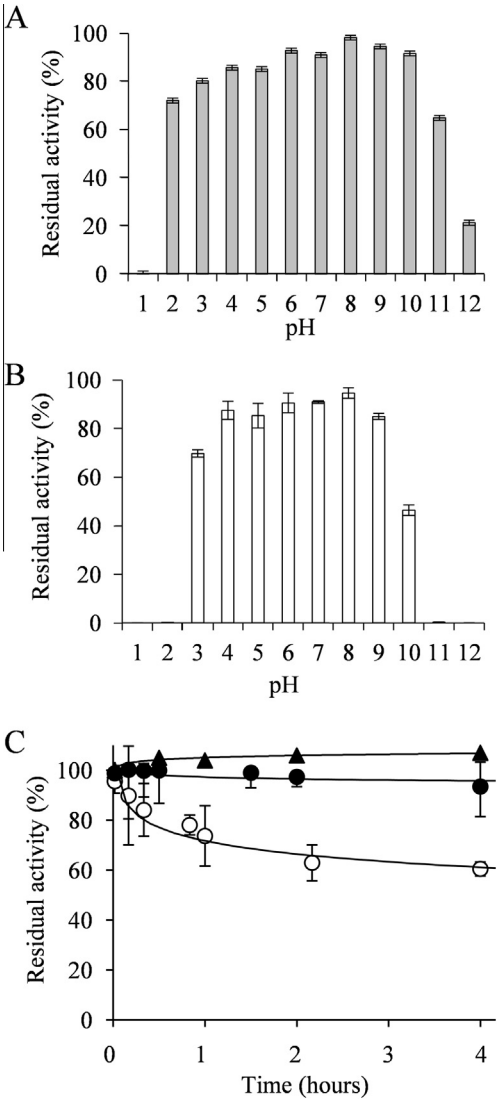

Fig. 4. pH stability of the purified DyP*. (A, B) Residual activities after 24 h incubation at different pH values measured at 4 °C and room temperature, respectively. (C) Time course of DyP* inactivation at pH 2.5 during incubation at 4 °C (black circles) and room temperature (white circles) and wild DyP from *A. auricula-judae* at room temperature (triangles). Error bars represent the standard deviations of the means of three measurements.

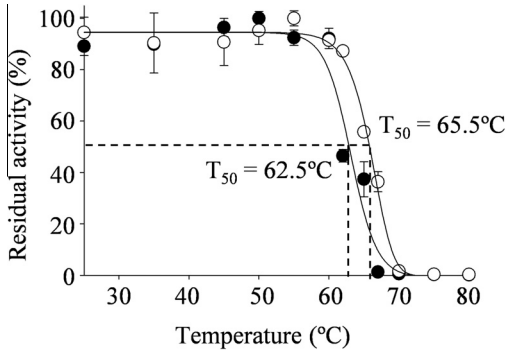

Fig. 5. Temperature stability of DyP* from *E. coli* (black) and wild DyP from fungal cultures (white). Residual activity after 10 min incubation at different temperatures is shown as percentage of the maximal activity obtained. Error bars represent the standard deviations of the means of three measurements.

Table 2
Kinetic constants (K_m (μM), k_{cat} (s^{-1}), and k_{cat}/K_m (s^{-1} mM^{-1})) of *E. coli* expressed DyP* and wild DyP from fungal cultures oxidizing different dyes and aromatic substrates.[a]

		DyP*	Wild DyP
Reactive Blue 19 (low turnover)	K_m	14 ± 2	6.5 ± 0.9
	k_{cat}	32 ± 3	32 ± 2
	k_{cat}/K_m	2200 ± 200	4800 ± 900
Reactive Blue 19 (high turnover)	K_m	90 ± 10	120 ± 20
	k_{cat}	224 ± 10	422 ± 40
	k_{cat}/K_m	2400 ± 180	3600 ± 340
ABTS	K_m	123 ± 7	283 ± 39
	k_{cat}	225 ± 3	654 ± 35
	k_{cat}/K_m	1800 ± 90	2300 ± 200
DMP (low turnover)	K_m	6 ± 0.5	6 ± 0.9
	k_{cat}	8 ± 0.2	11 ± 0.4
	k_{cat}/K_m	1350 ± 100	2000 ± 200
DMP (high turnover)	K_m	703 ± 60	1320 ± 130
	k_{cat}	120 ± 3	420 ± 20
	k_{cat}/K_m	200 ± 18	320 ± 30
Reactive Black 5	K_m	16 ± 2	30 ± 5
	k_{cat}	4.8 ± 0.2	10.6 ± 1.1
	k_{cat}/K_m	310 ± 20	400 ± 20
VA	K_m	–	–
	k_{cat}	–	–
	k_{cat}/K_m	0.10 ± 0	0.11 ± 0

[a] Kinetic constants obtained at optimal pH 3 (Reactive Black 5, ABTS and DMP), pH 3.5 (Reactive Blue 19) and suboptimal pH 2.5 (VA), including two sets of constants (corresponding to low and high turnover sites) for some substrates (see Fig. 7). Means and 95% confidence limits.

pH optimum and stability

The optimum pH was calculated for the fungal and the *E. coli* expressed enzymes with five different substrates, including the azo dye Reactive Black 5, the anthraquinone dye Reactive Blue 19, the low redox-potential dye ABTS, and the simple phenolic and non-phenolic aromatic compounds DMP and VA (data not shown). The pH profiles were very similar for both enzymes, showing an optimum pH of 3–4 for the phenolic and dye substrates but a lower pH (1.8) for VA. No activity was detected over pH 5 in the case of VA, and over pH 6 for the rest of the substrates.

For fungal class II peroxidases as for DyPs, acidic conditions are required for the optimum oxidative activity of the enzyme, with even more acidic pH optima (lower than 3) in the case of nonphenolic aromatic substrates as VA. In the same way, the optimum of VP for VA oxidation was found to be pH 3, decreased by more than 95%

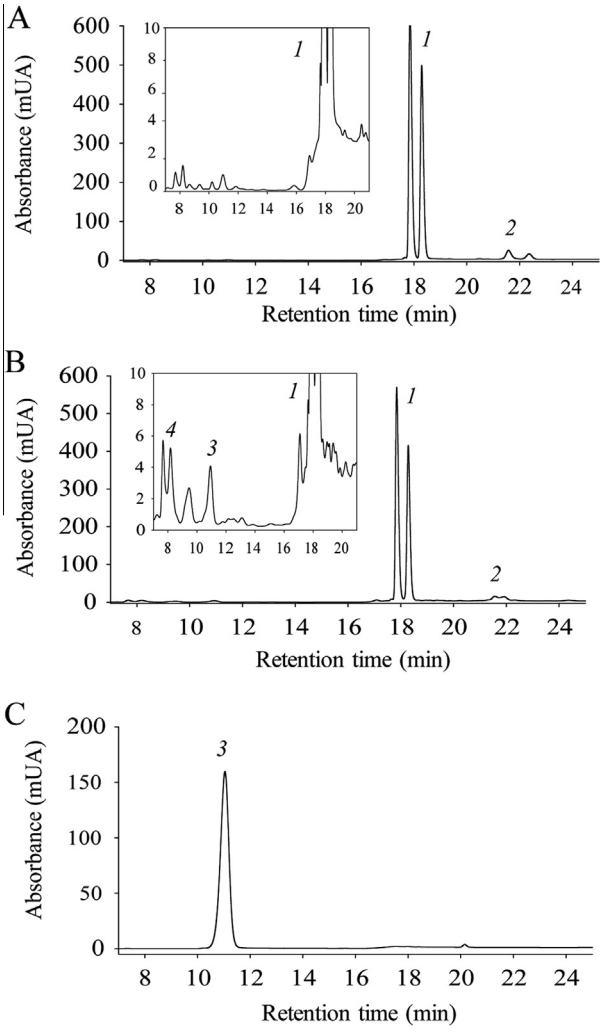

Fig. 6. Lignin model dimer degradation by DyP (HPLC analyses). (A) Control sample at initial reaction time (B). Partial degradation of racemic 4-*O*-methylsyringylglycerol β-guaiacyl ether (double peak 1 corresponding to the *erythro* and *threo* forms at 18.1 and 18.5 min, respectively) and a contaminant most probably corresponding to the ketone dimer (peak 2), and release of 3,4,5-trimethoxybenzaldehyde (peak 3 at 11.0 min) and other degradation products (4) during oxidation by DyP* (16 h) under H_2O_2 limiting conditions. The insets show amplifications (×60-fold) of the 7–21 min region. (C) 3,4,5-Trimethoxybenzaldehyde standard. The HPLC profiles were obtained at 255 nm.

when the pH increased from 3 to 4.5, and no activity was detectable at pH 5 [41]. Even some plant (class III) peroxidases showed slow VA oxidation activity when the pH was lowered, as reported for the acidic-pH-stable soybean peroxidase at pH 2.4 [42].

The study of the pH stability of DyP* was conducted incubating the enzyme for 24 h (at 4 and 25 °C) in a pH range from 1 to 12 (Fig. 4A and B). The enzyme turned out to be very stable towards high and low pH, although the stability decreased with increasing temperature. At 4 °C, DyP* maintained 72% and 80% of its initial activity after 24 h of incubation at pH 2 and 3, respectively. Something similar happened for high pH where the enzyme maintained 21% of its activity at pH 12 and 91% at pH 10. When the incubation was carried out at 25 °C, the residual activity of DyP* decreased to 70% at pH 3 and to 46% at pH 10, and no activity was detected at lower and higher pH values. To compare the pH stability of the *E. coli* DyP* with that of the wild DyP from the fungus, an assay at pH 2.5 was performed at 4 °C and room temperature (Fig. 4C). While the fungal DyP did not lose any activity within 4 h, the recombinant one (DyP*) lost 40% of its initial activity at room

temperature, highlighting the importance of the post-translational processing (glycosylation) of the fungal protein on its pH stability.

Temperature stability

The thermostability of DyP was examined by testing the reactivity towards ABTS after heat treatment of the enzyme at different temperatures. The stability to temperature was estimated for the recombinant and fungal enzymes. The maximum activities, taken as 100%, were detected at 55 °C for the *A. auricula-judae*-expressed DyP and at 50 °C for the recombinant *E. coli*-enzyme. Both enzymes were rather stable with T_{50} values of 62.5 and 65.5 °C, respectively (Fig. 5). These values are very similar to that reported for the *I. lacteus* DyP, whose T_{50} is 63 °C [27], but higher than those found for most basidiomycete peroxidases. For example (under similar conditions including 10 min incubation), the T_{50} values of *Pleurotus ostreatus* VPs and MnPs ranged from 53 to 63 °C and from 43 to 57 °C, respectively [43].

Catalytic properties

Wild and recombinant DyPs were tested on the five substrates described above and the obtained kinetic constants are shown in Table 2. Mn^{2+} oxidation was also assayed but no activity was detected. When both enzymes were compared, it was observed that there were no differences concerning the range of substrates they are able to oxidize, although DyP* showed lower catalytic efficiency than wild DyP for some of them due to slightly lower k_{cat} values. Some differences could be also observed between the catalytic constants here calculated and those previously published for the wild DyP purified from fungal cultures [26] probably due to: (i) differences in the pH used in the enzymatic assays; and (ii) the use of an erroneous molar extinction coefficient reported by Heinfling et al. for Reactive Black 5 [44] instead of that used here and in other studies [45,46].

As observed for other fungal DyPs, the highest activity of DyP* and wild DyP from *A. auricula-judae* was found for the anthraquinone dye (k_{cat} 224 and 422 s^{-1}, respectively) and ABTS (k_{cat} 225 and 654 s^{-1}) [7,27], followed by DMP (k_{cat} 120 and 420 s^{-1}) and the azo dye (k_{cat} 4.8 and 10 s^{-1}). Both enzymes exhibited a high apparent affinity (in the μM range) for Reactive Blue 19, Reactive Black 5, ABTS and DMP. By contrast, VA was oxidized with such low affinity that saturation was not observed and only the catalytic efficiency value (a second-order rate constant) for this substrate could be calculated. This value was always lower than those reported for well characterized ligninolytic class II peroxidases, being 2.7-fold lower than that described for VPs, isoenzymes 2 and 3, from *P. ostreatus* [43], 23-fold lower than that of VP1 from *P. ostreatus* and LiP1 from *Ceriporiopsis subvermispora* [47], and significantly lower (1200-fold) than that of LiP (isoenzyme H8) from *P. chrysosporium* [48]. Unlike VA, the DyP catalytic efficiency for ABTS oxidation was similar or even higher than that of fungal ligninolytic peroxides, including LiPs from *P. chrysosporium* and *C. subvermispora*, VPs from *P. eryngii* and *P. ostreatus*, and short MnPs

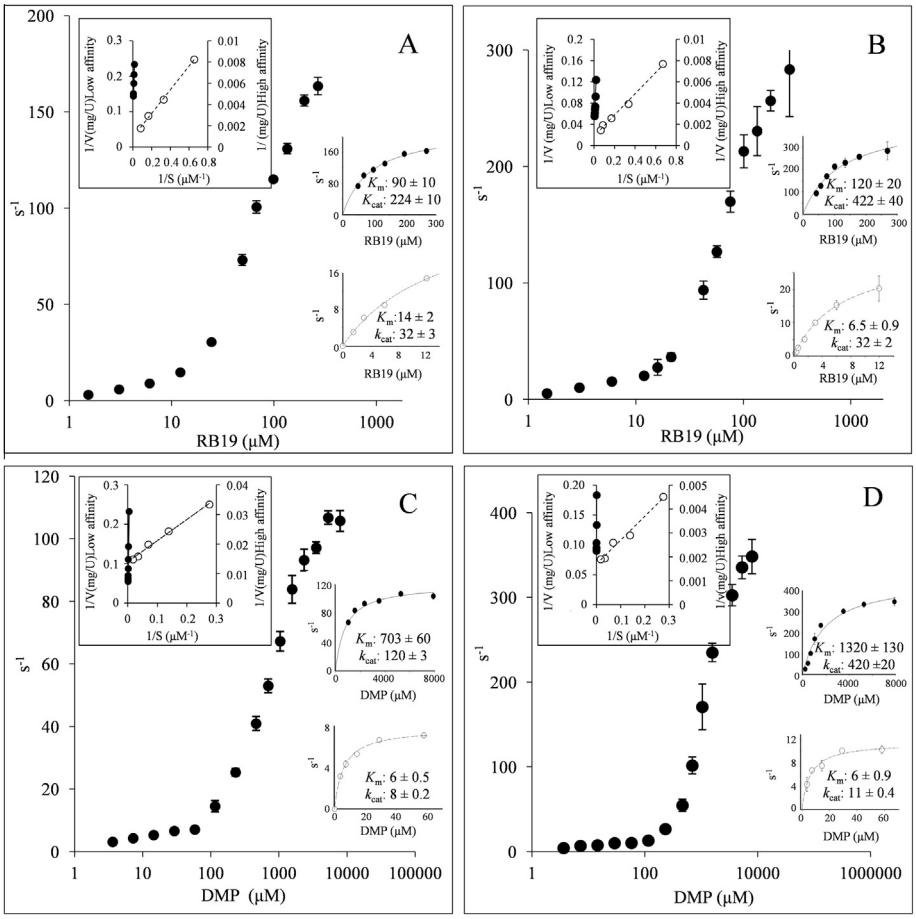

Fig. 7. Biphasic kinetics for Reactive Blue 19 (A, B) and DMP (C, D) oxidation by DyP* from *E. coli* (A, C) and wild DyP from fungal cultures (B, D). Double hyperbolic curves are shown with the *x* axis in logarithmic scale. The upper left insets illustrate the presence of high and low turnover sites as Lineweaver–Burk representations, and the right insets show the hyperbolic fits used to calculate the steady-state kinetic constants (their values also shown) for both oxidation sites.

from *P. ostreatus*. However, it was 2.8–6.8-fold lower for Reactive Black 5 oxidation than that of LiPs from *C. subvermispora* and VPs from *P. eryngii* and *P. ostreatus* [43,47,49].

Oxidation of adlerol (veratrylglycerol β-guaiacyl ether), a non-phenolic β-*O*-4 lignin model dimer, by wild DyP from *A. auricula-judae* was previously described by Liers et al. [26]. DyP* oxidation of a related lignin model dimer (4-*O*-methylsyringylglycerol β-guaiacyl ether) was investigated in presence of limiting H_2O_2 at pH 2.5, and analyzed by HPLC after 16 h of incubation (Fig. 6). The dimer was partially degraded, as shown by the decrease of the *erythro* (13%) and *threo* (18%) forms (double peak 1), and the release of 3,4,5-trimethoxybenzaldehyde (peak 3) resulting from C_α—C_β bond cleavage, with 34 μM final concentration representing 6% of the maximal yield according to the H_2O_2 concentration applied. Some small peaks (peak 4) appeared after the enzymatic treatment probably corresponding to other dimer degradation products [47], and peak 2 (a contamination of the model dimer) also decreased after the enzymatic treatment. The higher transformation of the *threo* isomer (compared with the *erythro* isomer) was in agreement with the preferential oxidation properties reported for both ligninolytic fungi [50] and their oxidative enzymes [51].

Interestingly, Reactive Blue 19 oxidation by wild and recombinant DyPs showed a biphasic (sigmoidal) kinetics enabling calculation of two sets of kinetic constants, and similar results were obtained for DMP oxidation (Table 2 and Fig. 7). This behavior can be related to the existence of more than one oxidation site with different turnover numbers and substrate affinities. In this respect, two K_m values were obtained for Reactive Blue 19 (14 and 90 μM) and DMP (6 and 700 μM) oxidation by DyP*, corresponding to different Reactive Blue 19 (32 and 224 s^{-1}, respectively) and DMP (8 and 120 s^{-1}, respectively) turnover numbers. A similar behavior has been reported for *P. eryngii* VP that can oxidize some phenols and dyes (such as DMP and ABTS) at a high and a low affinity site [52], which were localized at an exposed catalytic tryptophan [46] and at the main heme access channel [49], respectively. Future directed mutagenesis experiments and crystallographic studies using the DyP heterologous expression system developed here will help to clarify the presence of more than one oxidation site in this enzyme.

Acknowledgments

This work was supported by the INDOX (KBBE-2013-7-613549) project of the European Commission and the HIPOP (BIO2011-26694) project of the Spanish Ministry of Economy and Competitiveness (MINECO). F.J.R.-D. acknowledges a MINECO Ramón y Cajal contract. The authors thank J. Sipilä and P. Nousiainen (Helsinki University) for synthesizing the lignin model dimer used.

References

[1] K.G. Welinder, Superfamily of plant, fungal and bacterial peroxidases, Curr. Opin. Struct. Biol. 2 (1992) 388–393.
[2] M. Hofrichter, R. Ullrich, M.J. Pecyna, C. Liers, T. Lundell, New and classic families of secreted fungal heme peroxidases, Appl. Microbiol. Biotechnol. 87 (2010) 871–897.
[3] Y. Sugano, DyP-type peroxidases comprise a novel heme peroxidase family, Cell. Mol. Life Sci. 66 (2009) 1387–1403.
[4] B. Goblirsch, R.C. Kurker, B.R. Streit, C.M. Wilmot, J.L. Dubois, Chlorite dismutases, DyPs, and EfeB: 3 microbial heme enzyme families comprise the CDE structural superfamily, J. Mol. Biol. 408 (2011) 379–398.
[5] S.J. Kim, K. Ishikawa, M. Hirai, M. Shoda, Characteristics of a newly isolated fungus, *Geotrichum candidum* Dec 1, which decolorizes various dyes, J. Ferment. Bioeng. 79 (1995) 601–607.
[6] F.J. Ruiz-Dueñas, E. Fernández, M.J. Martínez, A.T. Martínez, *Pleurotus ostreatus* heme peroxidases: an *in silico* analysis from the genome sequence to the enzyme molecular structure, C. R. Biol. 334 (2011) 795–805.
[7] S.J. Kim, M. Shoda, Purification and characterization of a novel peroxidase from *Geotrichum candidum* Dec 1 involved in decolorization of dyes, Appl. Environ. Microbiol. 65 (1999) 1029–1035.
[8] Y. Sugano, K. Sasaki, M. Shoda, CDNA cloning and genetic analysis of a novel decolorizing enzyme, peroxidase gene *dyp* from *Geotrichum candidum* Dec 1, J. Biosci. Bioeng. 87 (1999) 411–417.
[9] Y. Sugano, C. Matsuo, M. Shoda, Efficient production of a heterologous peroxidase, DyP from *Geotrichum candidum* Dec 1, on solid-state culture of *Aspergillus oryzae* RD005, J. Biosci. Bioeng. 92 (2001) 594–597.
[10] Y. Sugano, Y. Ishii, M. Shoda, Role of H164 in a unique dye-decolorizing heme peroxidase DyP, Biochem. Biophys. Res. Commun. 322 (2004) 126–132.
[11] D. Floudas, M. Binder, R. Riley, K. Barry, R.A. Blanchette, B. Henrissat, A.T. Martínez, R. Otillar, J.W. Spatafora, J.S. Yadav, A. Aerts, I. Benoit, A. Boyd, A. Carlson, A. Copeland, P.M. Coutinho, R.P. de Vries, P. Ferreira, K. Findley, B. Foster, J. Gaskell, D. Glotzer, P. Górecki, J. Heitman, C. Hesse, C. Hori, K. Igarashi, J.A. Jurgens, N. Kallen, P. Kersten, A. Kohler, U. Kües, T.K.A. Kumar, A. Kuo, K. LaButti, L.F. Larrondo, E. Lindquist, A. Ling, V. Lombard, S. Lucas, T. Lundell, R. Martin, D.J. McLaughlin, I. Morgenstern, E. Morin, C. Murat, M. Nolan, R.A. Ohm, A. Patyshakuliyeva, A. Rokas, F.J. Ruiz-Dueñas, G. Sabat, A. Salamov, M. Samejima, J. Schmutz, J.C. Slot, F. St John, J. Stenlid, H. Sun, S. Sun, K. Syed, A. Tsang, A. Wiebenga, D. Young, A. Pisabarro, D.C. Eastwood, F. Martin, D. Cullen, I.V. Grigoriev, D.S. Hibbett, The Paleozoic origin of enzymatic lignin decomposition reconstructed from 31 fungal genomes, Science 336 (2012) 1715–1719.
[12] F.J. Ruiz-Dueñas, T. Lundell, D. Floudas, L.G. Nagy, J.M. Barrasa, D.S. Hibbett, A.T. Martínez, Lignin-degrading peroxidases in Polyporales: an evolutionary survey based on ten sequenced genomes, Mycologia 105 (2013) 1428–1444.
[13] C. Liers, M.J. Pecyna, H. Kellner, A. Worrich, H. Zorn, K.T. Steffen, M. Hofrichter, R. Ullrich, Substrate oxidation by dye-decolorizing peroxidases (DyPs) from wood- and litter-degrading agaricomycetes compared to other fungal and plant heme-peroxidases, Appl. Microbiol. Biotechnol. 87 (2013) 5839–5849.
[14] F.J. Ruiz-Dueñas, A.T. Martínez, Structural and functional features of peroxidases with a potential as industrial biocatalysts, in: E. Torres, M. Ayala (Eds.), Biocatalysts Based on Heme Peroxidases, Springer-Verlag, Berlin, 2010, pp. 37–59.
[15] D.I. Colpa, M.W. Fraaije, E. van Bloois, DyP-type peroxidases: a promising and versatile class of enzymes, J. Ind. Microbiol. Biotechnol. 41 (2014) 1–7.
[16] C. Zubieta, S.S. Krishna, M. Kapoor, P. Kozbial, D. McMullan, H.L. Axelrod, M.D. Miller, P. Abdubek, E. Ambing, T. Astakhova, D. Carlton, H.J. Chiu, T. Clayton, M.C. Deller, L. Duan, M.A. Elsliger, J. Feuerhelm, S.K. Grzechnik, J. Hale, E. Hampton, G.W. Han, L. Jaroszewski, K.K. Jin, H.E. Klock, M.W. Knuth, A. Kumar, D. Marciano, A.T. Morse, E. Nigoghossian, L. Okach, S. Oommachen, R. Reyes, C.L. Rife, P. Schimmel, B.H. van den, D. Weekes, A. White, Q. Xu, K.O. Hodgson, J. Wooley, A.M. Deacon, A. Godzik, S.A. Lesley, I.A. Wilson, Crystal structures of two novel dye-decolorizing peroxidases reveal a beta-barrel fold with a conserved heme-binding motif, Proteins 69 (2007) 223–233.
[17] H.J.O. Ogola, T. Kamiike, N. Hashimoto, H. Ashida, T. Ishikawa, H. Shibata, Y. Sawa, Molecular characterization of a novel peroxidase from the cyanobacterium *Anabaena* sp strain PCC 7120, Appl. Environ. Microbiol. 75 (2009) 7509–7518.
[18] X.H. Liu, Q. Du, Z. Wang, D.Y. Zhu, Y. Huang, N. Li, T.D. Wei, S.J. Xu, L.C. Gu, Crystal structure and biochemical features of EfeB/YcdB from *Escherichia coli* O157. Asp235 plays divergent roles in different enzyme-catalyzed processes, J. Biol. Chem. 286 (2011) 14922–14931.
[19] E. van Bloois, D.E.T. Pazmino, R.T. Winter, M.W. Fraaije, A robust and extracellular heme-containing peroxidase from *Thermobifida fusca* as prototype of a bacterial peroxidase superfamily, Appl. Microbiol. Biotechnol. 86 (2010) 1419–1430.
[20] J.N. Roberts, R. Singh, J.C. Grigg, M.E.P. Murphy, T.D.H. Bugg, L.D. Eltis, Characterization of dye-decolorizing peroxidases from *Rhodococcus jostii* RHA1, Biochemistry 50 (2011) 5108–5119.
[21] M.E. Brown, T. Barros, M.C.Y. Chang, Identification and characterization of a multifunctional dye peroxidase from a lignin-reactive bacterium, ACS Chem. Biol. 7 (2012) 2074–2081.
[22] J. Li, C. Liu, B.Z. Li, H.L. Yuan, J.S. Ang, B.W. Zheng, Identification and molecular characterization of a novel DyP-type peroxidase from *Pseudomonas aeruginosa* PKE117, Appl. Biochem. Biotechnol. 166 (2012) 774–785.
[23] A. Santos, S. Mendes, V. Brissos, L.O. Martins, New dye-decolorizing peroxidases from *Bacillus subtilis* and *Pseudomonas putida* MET94: towards biotechnological applications, Appl. Microbiol. Biotechnol. 98 (2014) 2053–2065.
[24] T. Johjima, M. Ohkuma, T. Kudo, Isolation and cDNA cloning of novel hydrogen peroxide-dependent phenol oxidase from the basidiomycete *Termitomyces albuminosus*, Appl. Microbiol. Biotechnol. 61 (2003) 220–225.
[25] M. Puhse, R.T. Szweda, Y.Y. Ma, C. Jeworrek, R. Winter, H. Zorn, *Marasmius scorodonius* extracellular dimeric peroxidase – exploring its temperature and pressure stability, BBA Protein Proteom. 1794 (2009) 1091–1098.
[26] C. Liers, C. Bobeth, M. Pecyna, R. Ullrich, M. Hofrichter, DyP-like peroxidases of the jelly fungus *Auricularia auricula-judae* oxidize nonphenolic lignin model compounds and high-redox potential dyes, Appl. Microbiol. Biotechnol. 85 (2010) 1869–1879.
[27] D. Salvachúa, A. Prieto, A.T. Martínez, M.J. Martínez, Characterization of a novel DyP-type peroxidase from *Irpex lacteus* and its application in the enzymatic hydrolysis of wheat straw, Appl. Environ. Microbiol. 79 (2013) 4316–4324.
[28] M. Puhse, R.T. Szweda, Y.Y. Ma, C. Jeworrek, R. Winter, H. Zorn, *Marasmius scorodonius* extracellular dimeric peroxidase – exploring its temperature and pressure stability, BBA Proteins Proteom. 1794 (2009) 1091–1098.
[29] E. Strittmatter, C. Liers, R. Ullrich, S. Wachter, M. Hofrichter, D.A. Plattner, K. Piontek, First crystal structure of a fungal high-redox potential dye-

decolorizing peroxidase: substrate interaction sites and long-range electron transfer, J. Biol. Chem. 288 (2013) 4095–4102.
[30] T. Yoshida, H. Tsuge, T. Hisabori, Y. Sugano, Crystal structures of dye-decolorizing peroxidase with ascorbic acid and 2,6-dimethoxyphenol, FEBS Lett. 586 (2012) 4351–4356.
[31] J. Hernández-Ruíz, J.N. Rodríguez-López, F. García-Canovas, M. Acosta, M.B. Arnao, Characterization of isoperoxidase-B2 inactivation in etiolated *Lupinus albus* hypocotyls, Biochim. Biophys. Acta – Protein Struct. Mol. Enzymol. 1478 (2000) 78–88.
[32] Y. Miki, M. Morales, F.J. Ruiz-Dueñas, M.J. Martínez, H. Wariishi, A.T. Martínez, *Escherichia coli* expression and in vitro activation of a unique ligninolytic peroxidase that has a catalytic tyrosine residue, Protein Expr. Purif. 68 (2009) 208–214.
[33] K. Zelena, H. Zorn, M. Nimtz, R.G. Berger, Heterologous expression of the *msp2* gene from *Marasmius scorodonius*, Arch. Microbiol. 191 (2009) 397–402.
[34] M. Pérez-Boada, W.A. Doyle, F.J. Ruiz-Dueñas, M.J. Martínez, A.T. Martínez, A.T. Smith, Expression of *Pleurotus eryngii* versatile peroxidase in *Escherichia coli* and optimisation of *in vitro* folding, Enzyme Microb. Technol. 30 (2002) 518–524.
[35] W.A. Doyle, A.T. Smith, Expression of lignin peroxidase H8 in *Escherichia coli*: Folding and activation of the recombinant enzyme with Ca^{2+} and haem, Biochem. J. 315 (1996) 15–19.
[36] A.T. Smith, N. Santama, S. Dacey, M. Edwards, R.C. Bray, R.N.F. Thorneley, J.F. Burke, Expression of a synthetic gene for horseradish peroxidase C in *Escherichia coli* and folding and activation of the recombinant enzyme with Ca^{2+} and heme, J. Biol. Chem. 265 (1990) 13335–13343.
[37] R. Whitwam, M. Tien, Heterologous expression and reconstitution of fungal Mn peroxidase, Arch. Biochem. Biophys. 333 (1996) 439–446.
[38] H.B. Dunford, Heme Peroxidases, Wiley-VCH, New York, 1999.
[39] B. Valderrama, R. Vazquez-Duhalt, Electron-balance during the oxidative self-inactivation of cytochrome c, J. Mol. Catal. B Enzym. 35 (2005) 41–44.
[40] A.N.P. Hiner, J. Hernández-Ruíz, F. García-Cánovas, A.T. Smith, M.B. Arnao, M. Acosta, A comparative study of the inactivation of wild-type, recombinant and two mutant horseradish peroxidase isoenzymes C by hydrogen peroxide and *m*-chloroperoxybenzoic acid, Eur. J. Biochem. 234 (1996) 506–512.
[41] M.J. Martínez, F.J. Ruiz-Dueñas, F. Guillén, A.T. Martínez, Purification and catalytic properties of two manganese-peroxidase isoenzymes from *Pleurotus eryngii*, Eur. J. Biochem. 237 (1996) 424–432.
[42] J.P. McEldoon, A.R. Pokora, J.S. Dordick, Lignin peroxidase-type activity of soybean peroxidase, Enzyme Microb. Technol. 17 (1995) 359–365.
[43] E. Fernández-Fueyo, F.J. Ruiz-Dueñas, M.J. Martínez, A. Romero, K.E. Hammel, F.J. Medrano, A.T. Martínez, Ligninolytic peroxidase genes in the oyster mushroom genome: heterologous expression, molecular structure, catalytic and stability properties and lignin-degrading ability, Biotechnol. Biofuels 7 (2014) 2.
[44] A. Heinfling, F.J. Ruiz-Dueñas, M.J. Martínez, M. Bergbauer, U. Szewzyk, A.T. Martínez, A study on reducing substrates of manganese-oxidizing peroxidases from *Pleurotus eryngii* and *Bjerkandera adusta*, FEBS Lett. 428 (1998) 141–146.
[45] D. Salvachúa, A. Prieto, A.T. Martínez, M.J. Martínez, Characterization of a novel dye-decolorizing peroxidase (DyP)-type enzyme from *Irpex lacteus* and its application in enzymatic hydrolysis of wheat straw, Appl. Environ. Microbiol. 79 (2013) 4316–4324.
[46] M. Pérez-Boada, F.J. Ruiz-Dueñas, R. Pogni, R. Basosi, T. Choinowski, M.J. Martínez, K. Piontek, A.T. Martínez, Versatile peroxidase oxidation of high redox potential aromatic compounds: site-directed mutagenesis, spectroscopic and crystallographic investigations of three long-range electron transfer pathways, J. Mol. Biol. 354 (2005) 385–402.
[47] E. Fernández-Fueyo, F.J. Ruiz-Dueñas, Y. Miki, M.J. Martínez, K.E. Hammel, A.T. Martínez, Lignin-degrading peroxidases from genome of selective ligninolytic fungus *Ceriporiopsis subvermispora*, J. Biol. Chem. 287 (2012) 16903–16916.
[48] W.A. Doyle, W. Blodig, N.C. Veitch, K. Piontek, A.T. Smith, Two substrate interaction sites in lignin peroxidase revealed by site-directed mutagenesis, Biochemistry 37 (1998) 15097–15105.
[49] M. Morales, M.J. Mate, A. Romero, M.J. Martínez, A.T. Martínez, F.J. Ruiz-Dueñas, Two oxidation sites for low redox-potential substrates: a directed mutagenesis, kinetic and crystallographic study on *Pleurotus eryngii* versatile peroxidase, J. Biol. Chem. 287 (2012) 41053–41067.
[50] C. Bohlin, K. Lundquist, L.J. Jonsson, Diastereomer selectivity in the degradation of a lignin model compound of the arylglycerol beta-aryl ether type by white-rot fungi, Enzyme Microb. Technol. 43 (2008) 199–204.
[51] C. Bohlin, K. Lundquist, L.J. Jonsson, Oxidation of the *erythro* and *threo* forms of the phenolic lignin model compound 1-(4-hydroxy-3-methoxyphenyl)-2-(2-methoxyphenoxy)-1,3-propanediol by laccases and model oxidants, Bioorg. Chem. 37 (2009) 143–148.
[52] F.J. Ruiz-Dueñas, M. Morales, E. García, Y. Miki, M.J. Martínez, A.T. Martínez, Substrate oxidation sites in versatile peroxidase and other basidiomycete peroxidases, J. Exp. Bot. 60 (2009) 441–452.